

Molecular Dynamics Simulation of Glass Forming Ability of Al₃₀Co₁₀ Amorphous Alloy

Chunping Fu, Lingtao Sun, Zhengfu Cheng

Department of Physics, Chongqing University of Arts and Sciences, Chongqing, China

Email: fuchunping@163.com

Received 2 August 2015; accepted 26 September 2015; published 29 September 2015

Copyright © 2015 by authors and Scientific Research Publishing Inc.

This work is licensed under the Creative Commons Attribution International License (CC BY).

<http://creativecommons.org/licenses/by/4.0/>



Open Access

Abstract

By using LAMMPS of the open source software, the micro-structures of Al₃₀Co₁₀ alloys were studied. Based on the average atomic volume, pair distribution function and bond-angle distribution functions, Honeycutt-Andersen (HA) bond-type index analysis shows that Al₃₀Co₁₀ alloy system begins to transform into a glass state with the temperature rapidly decreasing to 900 K. The process temperature is decreased from 900 K to 300 K, the radial distribution function $g(r)$ the first peak height with increased, width as decreasing temperature, and the system is an amorphous alloy when second peak appears obvious splitting. The bond angle distribution function showed second peaks when the temperature dropped to 300 K, so that the alloy atoms become orderly. Meanwhile the 1551 bond pairs increase to 35% with decreasing temperature; it implies that the Al₃₀Co₁₀ alloy system can be well transformed into the glass state.

Keywords

Al₃₀Co₁₀, Amorphous Alloy, Molecular Dynamics

1. Introduction

With the long-range disorder and short-range characteristics of amorphous alloy, it is also called the metallic glass (MGs). The amorphous alloys are of great interest owing to their unique combination of high specific strength and ductility, good corrosion resistance and abrasive resistance, representing an intriguing class of potential structural materials [1]-[8]. Since the first synthesis of amorphous phase of Au-Si alloy by rapid solidification in 1960 [1], active research on metallic glassy (MG) alloys has begun. Bulk MG alloys such as RE-Al-TM [2] (RE ¼ Sm, Y; TM ¼ Fe, Co, Cu), Cu-Zr-Ag [3], Fe-B-Si-Nb, and Cu-Cr-Hf [4] have been obtained and

well studied through conventional solidification method. Among the large number of MGs materials, bulk Al-based MGs have received increasing interest owing to their unique combination of high specific strength, low elastic modulus, good corrosion resistance, as well as low density, representing a promising engineering materials [5]-[7]. For the Al-based metallic glasses they are provided with low density and low elastic modulus, but can use the national defense and industrial applications, which have broad social value and economic value. Since Inoue [2] [3] [5] found successful multi-component bulk amorphous Alloy, over the past decades, the researchers have been able to prepare Al-based bulk amorphous alloys in the laboratory, such as Al-Cu, Al-Zr, Al-Ni-Zr amorphous alloys etc. Meanwhile, Co-based amorphous alloy is equipped with low coercivity, high magnetic permeability, the temperature stability, the excellent zero magnetostriction coefficient and so on; it's playing a more and more important role in the electronics and communications industries, and its application prospect is broad [9]-[23]. Therefore, we performed molecular dynamics (MD) simulations to study the glass formation of the liquid $\text{Al}_{30}\text{Co}_{10}$. It is hoped that more data will be provided for experiment by the molecular dynamics simulations to create the high temperature, high pressure and other extreme conditions.

In this article, we selected the Al as the main backing material to study the glass formation process and associated structural evolution by MD simulations. A detailed analysis of local atomic structure has been done during the glass formation of the amorphous $\text{Al}_{30}\text{Co}_{10}$ by various structural characterization methods, including pair distribution function [17] [18], bond-angle distribution function and Voronoi tessellation analysis [19] [20]. With these studies, we attempt to understand the factors controlling the formation of Al-based bulk metallic glasses (BMGs) by the viewpoint of the glass transition temperature (T_g) and micro-structures.

2. Simulation Methods

In this work, the MD simulation is carried out using the open code LAMMPS program [21]-[25]. The embedded atom method (EAM) is expressed as

$$U = \sum_i F(\rho_i) + \frac{1}{2} \sum_{\substack{i,j \\ (i \neq j)}} \phi(r_{ij}) \quad (1)$$

where ϕ_{ij} is the two-body central potential between atoms i and j within the separation distance r_{ij} , and $F(\rho_i)$ the embedding energy of atom with the electron density [23]-[25]. The present MD simulations have been carried out as an NPT isobaric-isothermal ensemble. The positions of atoms are calculated by the verlet algorithm. The time step was chosen to be 2 fs. the well-equilibrated initial system, including 4000 atoms distributed in a $10\text{a} \times 10\text{a} \times 10\text{a}$ lattice unit cubic box; which contains 3000 Al atoms and 1000 Co atoms, respectively. We gradually heat the system to 2200 K, and then let the system run 50,000 MD time steps (30 ps) at 2200 K to obtain a fully liquid state, and finally the liquid system was quenched to $T = 300$ K at the cooling rate of 5×10^{12} K/s. During the simulation processes, system volume is automatically adjusted to correspond to the given temperature and zero pressure conditions.

3. Results and Discussions

As is known that the Liquid transform to crystalline state is a first order phase transformation; it is typical of the System volume will be sudden changes in the crystalline temperature. **Figure 1** represents the variation of average volume of per atom as a function of temperature during the heating and cooling processes with the cooling rate of 5×10^{12} K/s. As shown in **Figure 1**, there is an obvious jump in the volume versus temperature curve (black curve) near the 900 K With the rapid decrease of temperature. in the cooling process, it is found that the liquid-crystal is not transform to amorphous state with temperature decreasing form 2300 K to 1000 K if the the system volume will not be Sudden changes; however, representing the typical character of a liquid-glass transition is the system volume Sudden changes at the temperature region near T_g , one can yield a crossover at which the T_g was determined to be 900 K. In other words, the system of $\text{Al}_{30}\text{Co}_{10}$ liquid alloy will be transform to amorphous with the $T_g = 900\text{K}$.

It is one of the most important function, revealing the structural characteristics of the system as Pair distribution function (PDF) analysis, most particularly for amorphous and liquids systems. The Pair distribution function (PDF) is defined by the probability of finding an atom in the spherical shell where particle i is taken as the center. Expressed in a formula, this law can be written as follows.

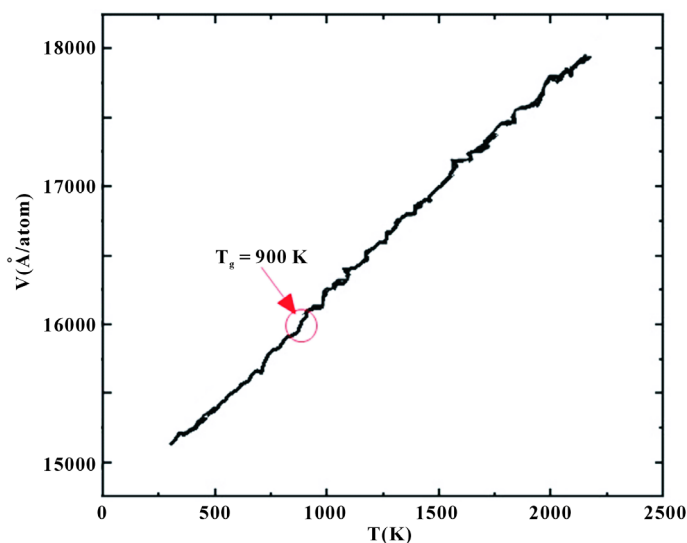


Figure 1. The volume as a function of the temperature for $\text{Al}_{30}\text{Co}_{10}$ alloy.

$$g(r) = 4\pi r^2 \rho(r) dr \quad (2)$$

where $\rho(r)$ the number of atoms around a central atom within the distance interval between r and $r + dr$, which is atomic average statistical distribution. By simulating the PDF of the liquid Al, we found that the PDF of the liquid Al are good agreement with the experimental data (Ref. 84) as shown in **Figure 2**; and calculating data represented by curve line and the circles represented experimental data.

In liquid system, atoms do as random motion, which cannot be described by the fixed coordinate; we compared the PDF for the liquid system with amorphous state, it is seen that the PDF are very similar in almost every way. However, the atom can be vibrate in a certain range in amorphous, which can be described by the fixed coordinate; the first peak of the PDF is relatively narrow and sharp; the second peak will be split into two peaks, which one peak is higher than the other peaks, which hump shaped is also one of the most important judgement of amorphous typical characteristics.

The PDF are shown in **Figure 3**. We select six temperatures (2100, 1800, 1500, 1200, 900, 600, and 300 K) to illuminate the rapid solidification process of the $\text{Al}_{30}\text{Co}_{10}$ liquid alloy. It can be seen that the first peak of PDF gets higher as the temperature decreases, which means that atomic ordering in the first coordination shell increases as the temperature decreases. The second and third broad peaks become more pronounced as the temperature decreases to 1200 K. Meanwhile the temperature decreases to 900 K, the second peak start to splits into a tiny peak at the right; and then the second peak splits into two obvious sub peaks when the temperature further decreases to 300 K. In summary, the system of $\text{Al}_{30}\text{Co}_{10}$ liquid alloy were start to transform to amorphous at the temperature decreases to 900 K, which is accord to the upward analysis that the T_g of the simulated system is 900 K.

In amorphous system, the local structure was more comprehensive described by bond-angle distribution functions. Every barber knows that if a system is dominated by icosahedral structures, there will be the two main peaks at 63.4 and 113.4 in bond-angle distribution functions for the cluster structures in the system; meanwhile, there will be obvious degrees of 60, 90 and 120 in bond-angle distribution functions, it is shows that the FCC or HCP system are dominate in the system. For **Figure 4**, we can see that the seven curves the main angle angles distribute in the vicinity of 60 and 120, not 90 with decreasing temperature at the cooling rate of 5×10^{12} K/s, the capacity of degrees in the vicinity of 60 and 120 has obvious increased with the decrease of temperature; it is obvious that the angle degrees tend to be about 63.4 and 113.4, which means that the dominated local structures are icosahedral structures in the amorphous Al-Co system.

Furthermore, we get more information about micro-structures of $\text{Al}_{30}\text{Co}_{10}$ alloy, which is analyzed using the Honeycutt-Andersen (HA) bond-type index and give a detailed three-dimensional image of the local configurations in the cooling process. The HA bond-type index is able to give information about the number and properties of common nearest neighbors of each atom pair which can be used to characterize the local environment

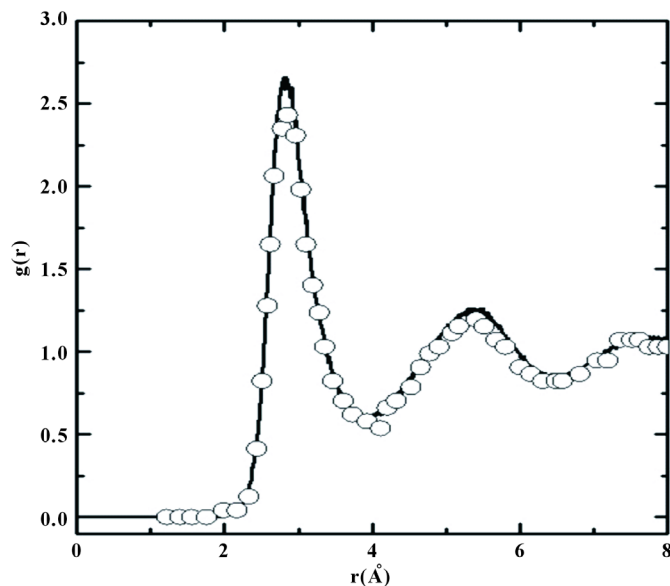


Figure 2. The calculated pair-correlation functions of liquid $\text{Al}_{30}\text{Ti}_{10}$ at temperature 2000 k with the available data.

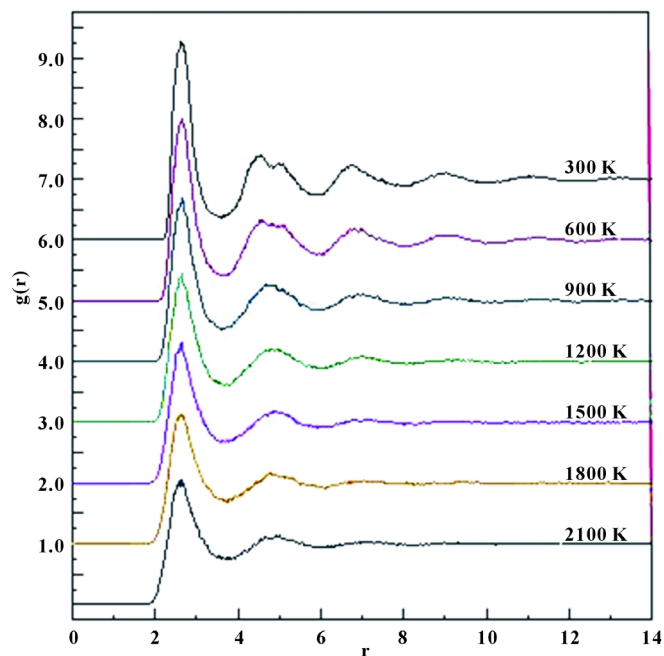


Figure 3. The $g(r)$ for $\text{Al}_{30}\text{Co}_{10}$ alloy between 2100 and 300 K at 300 K intervals.

surrounding atomic pair under consideration. Each pair of atoms is classified by the relation among their neighbors with four indices of integer. The first integer indicates whether the considered atomic pair is closer than a specified cutoff distance, chosen to be the nearest-neighbor distance determined by the first valley in the pair correlation function. If the pair is bonded, the first integer is 1, or else, 2. The second integer is the common-neighbor number of the considered pair; the third represents the number of bonds among the common neighbors; the fourth is used to distinguish the atomic pair when the former three integers are not sufficient. While, the some pairs of 1551, 1541, 1431 types are shown because they represented local icosahedron and defect icosahedron, respectively. As shown in **Figure 5**, it can be seen that the 1551, 1541, 1431 pairs have fraction of 5%,

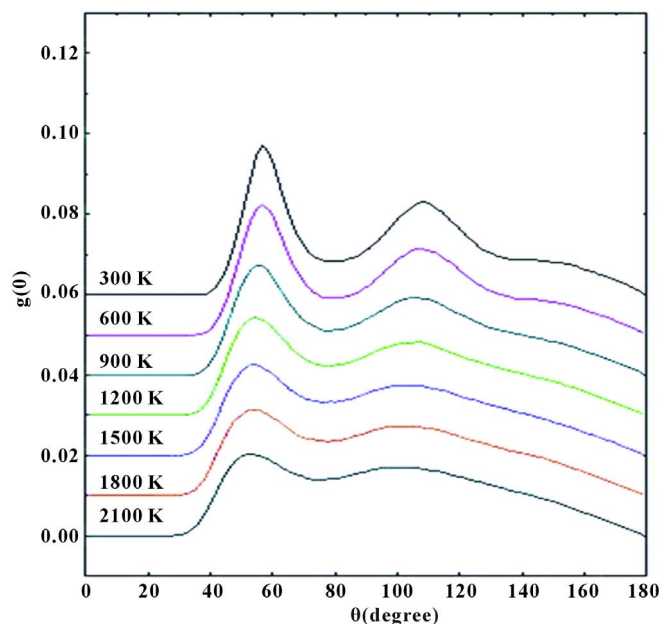


Figure 4. Bond-angle distribution function of $\text{Al}_{30}\text{Co}_{10}$ alloy at the different temperatures.

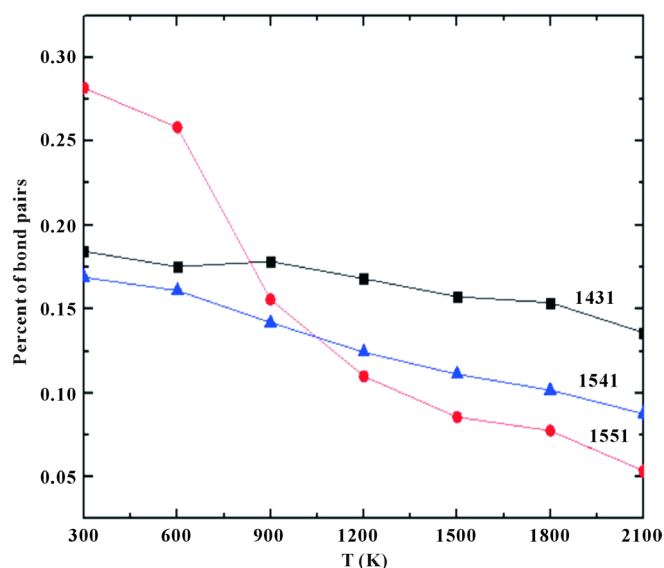


Figure 5. Some Honeycutt-Andersen (HA) indices as a function of the temperatures for $\text{Al}_{30}\text{Co}_{10}$ alloy.

8.5%, 13% at the temperature of 2100 K, respectively. For the 1551 pairs, the fraction increased from 5% to 27.5% with temperature rapidly decreasing from 2100 K to 300 K. The fraction of 1551 pairs, a modest figure, with the temperature of decreasing from 2100 K to 900 K; however, it was booming growth to 27.5% when the temperature of decreasing from 900 K to 300 K because the system have started to transform to amorphous at 900 K. The fraction of 1431 pair did not change much, while increasing from 13% to 15.7% in the whole temperature range; the fraction of 1541 pairs is 14.6% at 300 K.

4. Conclusion

We presented the results of an MD study of the glass transition for $\text{Al}_{30}\text{Co}_{10}$. The pair correlation function,

bond-angle distribution functions and HA bond-type index at different temperatures are obtained by our simulation. The PDF illustrates that the shortage of medium structure orderings is enhanced with decreasing temperature. Meanwhile, when the temperature decreases to 900 K, the second peak starts to split into a tiny peak at the right, and then the second peak splits into two obvious sub peaks when the temperature further decreases to 300 K. In summary, the system of Al₃₀Co₁₀ liquid alloy starts to transform into amorphous alloys when the temperature decreases to 900 K, which is according to the upward analysis that the T_g of the simulated system is 900 K. The HA bond-type result shows that the local icosahedron and defect icosahedron are decreased in cooled alloy liquid during the rapid solidification processes, while the 1551 pairs, the fraction increases from 5% to 27.5% with temperature rapidly decreasing from 2100 K to 300 K.

Acknowledgements

The authors thank the financial support of the Natural Science Foundation of Yong Chuan (Grant 2014nc4002) and the foundation of Chongqing University of Arts and Science (Grants Z2013KJ17).

References

- [1] Johnson, W.L. and Bull, M.R. (1999) Bulk Glass-Forming Metallic Alloys. *Science and Technology*, **24**, 42-56.
- [2] Inoue, A. and Takaomi, I. (1998) Soft Magnetic of Co-Based Amorphous Alloys with Wide Super-Cooled Liquid Region. *Materials Transactions Jim*, **39**, 762-770.
- [3] Inoue, A. (1995) High Strength Bulk Amorphous Alloys with Low Critical Cooling Rates. *Materials Transactions Jim*, **36**, 866-875. <http://dx.doi.org/10.2320/matertrans1989.36.866>
- [4] Sun, Y.L., Qu, D.D. and Sun, Y.J. (2010) Inhomogeneous Structure and Glass-Forming Ability in Zr-Based Bulk Metallic Glasses. *Journal of Non-Crystalline Solids*, **356**, 39-45. <http://dx.doi.org/10.1016/j.jnoncrysol.2009.09.021>
- [5] Inoue, A. (2000) Stabilization of Metallic Super Cooled Liquid and Bulk Amorphous Alloys. *Acta Materialia*, **48**, 279-306. [http://dx.doi.org/10.1016/S1359-6454\(99\)00300-6](http://dx.doi.org/10.1016/S1359-6454(99)00300-6)
- [6] Xia, J.H., Cheng, Z.F. and Cao, Y.J. (2012) Molecular Dynamics Simulation of Microstructure Evolution in Ti₇₅Al₂₅ Alloys. *J. At. Mol. Phys.*, **29**, 739-745.
- [7] Cheng, Y.Q., Ma, E. and Sheng, H.W. (2009) Atomic Level Structure in Multi-Component Bulk Metallic Glass. *Physical Review Letters*, **102**, Article ID: 245501. <http://dx.doi.org/10.1103/PhysRevLett.102.245501>
- [8] Li, G.X., Liang, Y.F., Zhu, Z.G. and Liu, C.S. (2003) Microstructural Analysis of the Radial Distribution Function for Liquid and Amorphous Al. *Journal of Physics: Condensed Matter*, **15**, 2259-2267. <http://dx.doi.org/10.1088/0953-8984/15/14/302>
- [9] Daw, M.S. and Baskes, M.I. (1983) Semiempirical, Quantum Mechanical Calculation of Hydrogen Embrittlement in Metals. *Physical Review Letters*, **50**, 1285. <http://dx.doi.org/10.1103/PhysRevLett.50.1285>
- [10] Liu, C.S., Xia, J., Zhu, Z.G. and Sun, D.Y. (2001) The Cooling Rate Dependence of Crystallization for Liquid Copper: A Molecular Dynamic Simulation. *The Journal of Chemical Physics*, **114**, 7506-7513. <http://dx.doi.org/10.1063/1.1362292>
- [11] Cheng, Y.Q., Ma, E. and Sheng, H.W. (2009) Atomic Level Structure in Multicomponent Bulk Metallic Glass. *Physical Review Letters*, **102**, Article ID: 245501. <http://dx.doi.org/10.1103/PhysRevLett.102.245501>
- [12] Zope, R.R. and Mishin, Y. (2003) Inter-Atomic Potentials for Atomistic Simulations of the Ti-Al System. *Physical Review B*, **68**, Article ID: 024102. <http://dx.doi.org/10.1103/PhysRevB.68.024102>
- [13] Dang, S.E., Zhang, X.H., Yan, Z.J., Hu, Y. and Hao, W.X. (2007) Correlation between Crystallization Kinetics of Amorphous Alloys and Primary Phases during Crystallization. *The Chinese Journal of Nonferrous Metals*, **17**, 296-302.
- [14] Fan, G.J., Loser, W., Routh, S. and Eckert, J. (2000) Glass-Forming Ability of RE-Al-TM Alloys (RE=Sm, Y; TM=Fe, Co, Cu). *Acta Materialia*, **48**, 3823-3831. [http://dx.doi.org/10.1016/S1359-6454\(00\)00195-6](http://dx.doi.org/10.1016/S1359-6454(00)00195-6)
- [15] Pei, X.Q., Lu, C. and Lee, H.P. (2005) Crystallization of Amorphous Alloy Isothermal Annealing: A Molecular Dynamics Study. *Journal of Physics: Condensed Matter*, **17**, 1493-1504. <http://dx.doi.org/10.1088/0953-8984/17/10/006>
- [16] Launey, M.E., Busch, R. and Kruzic, J.J. (2008) Effects of Free Volume Changes and Residual Stresses on the Fatigue and Fracture Behavior of a Zr-Ti-Ni-Cu-Be Bulk Metallic Glass. *Acta Materialia*, **56**, 500-510. <http://dx.doi.org/10.1016/j.actamat.2007.10.007>
- [17] Klement, W., Willens, R.H. and Duwez, P. (1960) Non-Crystalline Structure in Solidified Gold-Silicon Alloys. *Nature*,

- 187**, 869-870. <http://dx.doi.org/10.1038/187869b0>
- [18] Sheng, H.W., Liu, H.Z., Cheng, Y.Q., Wen, J., Lee, P.L., Luo, W.K., Shastri, S.D. and Ma, E. (2007) Polyamorphism in a Metallic Glass. *Nature Materials*, **6**, 192-197. <http://dx.doi.org/10.1038/nmat1839>
- [19] Allen, M.P. and Tildesley, D.J. (1987) *Computer Simulation of Liquids*. Oxford University Press, Oxford.
- [20] Waseda, Y. (1980) *The Structure of Non-Crystalline Materials*. McGraw-Hill, New York.
- [21] Finney, J.L. (1977) Modeling Structures of Amorphous Metals and Alloys. *Nature*, **266**, 309-314. <http://dx.doi.org/10.1038/266309a0>
- [22] Finney, J.L. (1970) Random Packings and the Structure of Simple Liquids. II. The Molecular Geometry of Simple Liquids. *Proceedings of the Royal Society A: Mathematical, Physical and Engineering Sciences*, **319**, 495-507. <http://dx.doi.org/10.1098/rspa.1970.0190>
- [23] Mei, J. and Davenport, J.W. (1992) Free-Energy Calculations and the Melting Point of Al. *Physical Review B*, **46**, Article ID: 21. <http://dx.doi.org/10.1103/PhysRevB.46.21>
- [24] Daw, M.S. and Baskes, M.I. (1983) Semiempirical, Quantum Mechanical Calculation of Hydrogen Embrittlement in Metals. *Physical Review Letters*, **85**, Article ID: 1285. <http://dx.doi.org/10.1103/PhysRevLett.50.1285>
- [25] Rifkin, J. (2002) XMD-Molecular Dynamics Program. Version 2.5.32, University of Connecticut, Storrs.